PNAS RESEARCH ARTICLE | MEDICAL SCIENCES OPEN ACCESS

Elevated *BICD2* DNA methylation in blood of major depressive disorder patients and reduction of depressive-like behaviors in hippocampal *Bicd2*-knockdown mice

Jianbo Xiu[a,b,1], Jiayu Li[a,b,1], Zeyue Liu[a,b,1], Hui Wei[a,b], Caiyun Zhu[a,b], Rongrong Han[a,b], Zijing Liu[a,b], Wanwan Zhu[a,b], Yan Shen[a,b], and Qi Xu[a,b,2]

Edited by Joseph Takahashi, University of Texas Southwestern Medical Center, Dallas, TX; received February 3, 2022; accepted June 7, 2022

Major depressive disorder (MDD) is a prevalent and devastating mental illness. To date, the diagnosis of MDD is largely dependent on clinical interviews and questionnaires and still lacks a reliable biomarker. DNA methylation has a stable and reversible nature and is likely associated with the course and therapeutic efficacy of complex diseases, which may play an important role in the etiology of a disease. Here, we identified and validated a DNA methylation biomarker for MDD from four independent cohorts of the Chinese Han population. First, we integrated the analysis of the DNA methylation microarray ($n = 80$) and RNA expression microarray data ($n = 40$) and identified *BICD2* as the top-ranked gene. In the replication phase, we employed the Sequenom MassARRAY method to confirm the DNA hypermethylation change in a large sample size ($n = 1{,}346$) and used the methylation-sensitive restriction enzymes and a quantitative PCR approach (MSE-qPCR) and qPCR method to confirm the correlation between DNA hypermethylation and mRNA down-regulation of *BICD2* ($n = 60$). The results were replicated in the peripheral blood of mice with depressive-like behaviors, while in the hippocampus of mice, *Bicd2* showed DNA hypomethylation and mRNA/protein up-regulation. Hippocampal *Bicd2* knockdown demonstrates antidepressant action in the chronic unpredictable mild stress (CUMS) mouse model of depression, which may be mediated by increased BDNF expression. Our study identified a potential DNA methylation biomarker and investigated its functional implications, which could be exploited to improve the diagnosis and treatment of MDD.

major depressive disorder | DNA methylation | BICD2 | hippocampus | BDNF

Significance

To date, numerous studies have established the association of DNA methylation with MDD, but a reliable biomarker with consistent results across different studies has not been available. In our study, we identified *BICD2* as a new gene associated with MDD and validated the *BICD2* association in four independent cohorts of the Chinese Han population to illustrate a potential of the diagnosis and treatment of MDD. We report the association of *BICD2* DNA methylation with MDD and the functional consequences of its altered expression in an animal model of depression.

Major depressive disorder (MDD) is a mental health condition characterized by persistent feelings of sadness and loss of interest or pleasure and also a leading cause of disability around the world (1), with an estimated 12-mo prevalence of 6% (2). To date, the diagnosis of MDD is largely dependent on clinical interviews and questionnaires. The lack of a reliable biomarker for MDD limits the confirmation of diagnosis, as well as the assessment of treatment and prognosis. A potential biomarker may also serve as a probe for elucidating the pathogenesis of disease or a target for developing new therapeutic interventions (3).

Although substantial progress has been made in understanding the neurobiology of depression, much work remains to be done, especially identification of validated biomarkers, detailed etiology, and effective treatments. MDD is a complex malady that is determined by the interactions between genetic, environmental, and epigenetic factors (4). The heritability of MDD estimated from twin studies is ∼30 to 40% (5). Recently, genome-wide association studies with large cohorts have identified several genetic risk variants associated with MDD (6, 7). While the identified variants only contribute to a very small proportion of the disease etiology (8), the biological functions of these variants and their interactions with epigenetic or environmental risk factors remain to be investigated. It is also worth noting that differences in ethnicity may contribute to poor replication of initial findings from different cohorts (6, 7). Stress is one of the main environmental factors triggering the onset of depression. The biological impact of stress is embedded in changes in epigenetic modifications and gene expression (9).

DNA methylation, as a major form of epigenetic modification, has long been known to regulate gene expression, further modulating diverse aspects of life functions (10). It is stable but reversible, thus providing a possibility to serve as a biomarker for the diagnosis and response to disease treatment. Indeed, blood-based DNA methylation assays have been used in the early detection and early relapse prediction of colorectal cancer (11). However, there is still no validated biomarker available for MDD. Although numerous studies using a candidate gene strategy have confirmed that changes in DNA methylation of *BDNF* and *SLC6A4* are associated with MDD (12), these results are

Author affiliations: [a]State Key Laboratory of Medical Molecular Biology, Institute of Basic Medical Sciences, Chinese Academy of Medical Sciences, School of Basic Medicine Peking Union Medical College, Beijing 100005, China; and [b]Neuroscience Center, Chinese Academy of Medical Sciences, Beijing 100005, China

Author contributions: J.X. and Q.X. designed research; J.X., J.L., Zeyue Liu, R.H., and Zijing Liu performed research; H.W. and W.Z. contributed new reagents/analytic tools; J.X., J.L., Zeyue Liu, H.W., and C.Z. analyzed data; and J.X., J.L., Y.S., and Q.X. wrote the paper.

The authors declare no competing interest.

This article is a PNAS Direct Submission.

[1]J.X., J.L., and Zeyue Liu contributed equally to this work.

[2]To whom correspondence may be addressed. Email: xuqi@pumc.edu.cn.

This article contains supporting information online at http://www.pnas.org/lookup/suppl/doi:10.1073/pnas.2201967119/-/DCSupplemental.

Published July 18, 2022.

rarely replicated in methylome-wide association studies (MWAS) (13–22). On the other hand, the top-ranked differentially methylated genes uncovered by the MWAS strategy also rarely overlap, possibly due to differences in the sample compositions (size, tissue, age, sex, ethnicity, etc.), detection methods, and statistical analysis. Therefore, multiple levels of validation within the same study are required to find a reliable biomarker. Findings from both candidate gene and MWAS strategies implicate that DNA methylation may be associated with antidepressant responses (12, 23, 24). This implies that manipulating DNA methylation may have therapeutic effects on MDD, as suggested by cancer research (25). In fact, the activity of DNA methyltransferases regulates emotional behavior and spine plasticity in the mouse nucleus accumbens (26) and mediates epigenetic effects of the antidepressant paroxetine (27). However, few studies have investigated whether a specific gene with altered DNA methylation in MDD could be exploited as a potential target for the development of alternative antidepressant therapy.

The principal aim of the current study was to identify and validate a DNA methylation biomarker for MDD in four independent cohorts of the Chinese Han population (Fig. 1*A*). We integrated the analysis of the DNA methylation microarray and RNA expression microarray data, and identified *BICD2* as the top-ranked gene. In the replication phase, we used the Sequenom MassARRAY method to confirm the DNA methylation change in a large sample and employed the methylation-sensitive restriction enzymes and a quantitative PCR approach (MSE-qPCR) and qPCR method to confirm the correlation between DNA methylation and mRNA expression of *BICD2*. Due to the limited access to postmortem brain tissues of MDD patients, we used a cross-species strategy to investigate the phenotype and function of *Bicd2* in a mouse model of depression.

Results

Genome-Wide Profiling of the DNA Methylome and Transcriptome in the Peripheral Blood of MDD Patients. The genome-wide patterns of DNA methylation in whole blood were assessed on Illumina Human Methylation 450 (HM450) bead chip microarrays from 40 MDD patients and 40 healthy controls (HCs) (the first cohort). HM450 can assay over 480 K CpG sites with

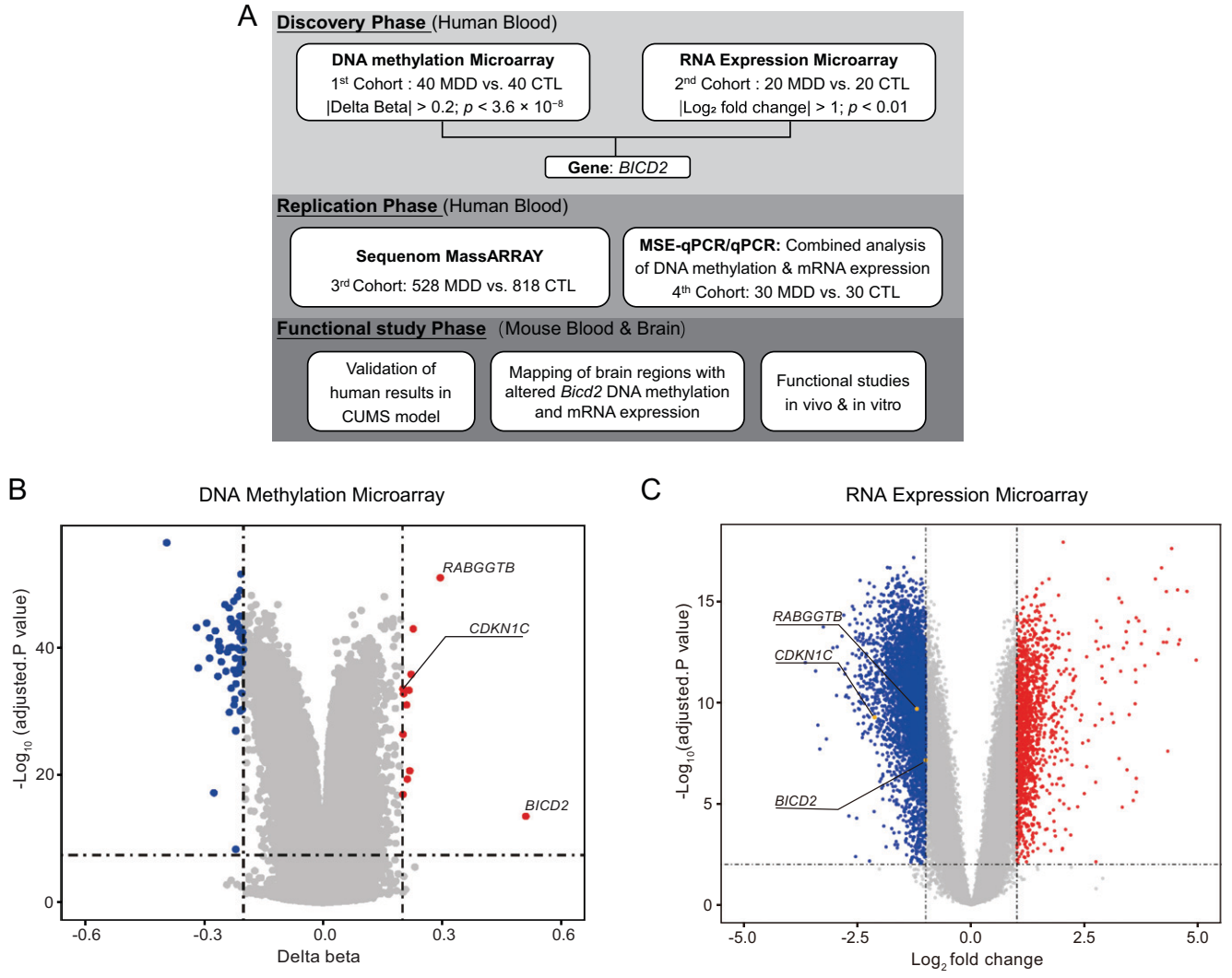

Fig. 1. Genome-wide profiling of the DNA methylome and transcriptome in the peripheral blood of MDD patients. (*A*) Diagram of the study design: The three research phases are presented. (*B*) Volcano plot for differential DNA methylation analysis of all CpG sites in MDD patients and healthy controls (CTL). Vertical and horizontal dashed lines represent the thresholds for discovering DMPs (absolute delta beta value >0.2, *P* value $<3.6 \times 10^{-8}$). Red dots indicate hypermethylated sites in MDD patients compared with CTL, and blue dots indicate hypomethylated sites. (*C*) Volcano plot for differential expression analysis between MDD patients and CTL. Vertical and horizontal dashed lines represent the thresholds for discovering differentially expressed genes (absolute Log_2 fold change >1 and *P* value <0.01). Red dots indicate up-regulated genes compared with CTL, and blue dots indicate down-regulated genes.

bisulfite-converted genomic DNA (Illumina, 2011) and has been widely used in MWAS (13–18). As shown in the volcano plot (Fig. 1*B* and Dataset S1), we identified 12 hypermethylated and 62 hypomethylated CpG sites covering 55 genes using a stringent threshold with absolute delta beta (Δβ) value >0.2 and *P* value $<3.6 \times 10^{-8}$. The Δβ value for each probe indicates the difference in mean DNA methylation between MDD patients and HCs. The *P* value has been estimated to be a significance threshold for epigenome-wide association studies (28). Microarray analysis of gene expression in whole blood was employed to reveal the potential functional consequences of differentially methylated genes from another cohort of 20 MDD patients and 20 healthy controls (the second cohort). As shown in the volcano plot (Fig. 1*C*) and Dataset S2, a total of 5,575 genes with absolute Log_2 fold change >1 and *P* value <0.01 were identified, 1,357 of which were up-regulated and 4,218 down-regulated. Integrated analysis of DNA methylome and transcriptome data uncovered that only three genes, *BICD2* (bicaudal D cargo adaptor 2), *RABGGTB* (Rab geranylgeranyltransferase subunit beta), and *CDKN1C* (cyclin-dependent kinase inhibitor 1C) showed DNA hypermethylation and mRNA down-regulation according to the above-mentioned filter criteria (Fig. 1*B* and *C* and Datasets S1 and S2). HM450 contains 24 CpG sites in the *BICD2* gene. There were four probes affiliated with the transcription start site, 13 in the gene body, and seven in the 3′ UTR. Only *cg14341177* in the 3′ UTR demonstrated an absolute Δβ value greater than 0.2 in the 24 CpG probes of *BICD2* and showed the largest change in DNA methylation among all HM450 probes (Δβ = 0.509722; *P* = 2.93E-14). When the DNA methylation microarray data were adjusted for age, cg14341177 was still the most differentially methylated site using the same threshold (Δβ = 0.509722, *P* = 6.41E-11; *SI Appendix*, Fig. S1 and Dataset S3) BICD2 is a dynein-activating adaptor protein involved in cargo transport (29) and organelle positioning (30–32). It plays critical roles in regulating neuronal migration (33–36). Multiple mutations have been found in *BICD2* associated with spinal muscular atrophy (37). *Bicd2* knockout mice show severe hydrocephalus and abnormal laminar organization, indicating a vital function in neural development (33). Therefore, we focused on *BICD2* in this work.

Replication of the *BICD2*-Associated Differentially Methylated Region and Its Correlation with mRNA Expression. Next, we employed the Sequenom MassArray approach to validate the HM450 results of *BICD2* from 528 MDD patients and 818 healthy controls (the third cohort). That is a mass spectrometry–based bisulfite sequencing method (38) that enables a region-specific DNA methylation assay and is suitable for high throughput analysis of regions of candidate genes or sites from MWAS. We performed Sequenom MassArray DNA methylation analysis on the 3′ UTR of *BICD2* with an amplicon and detected seven CpG units (Fig. 2*A*). A linear regression model was used to analyze the differences in DNA methylation between MDD patients and healthy controls adjusted for gender and age. The CpG_5 site, corresponding to *cg14341177* identified by the previous DNA methylation microarray analysis, was significantly hypermethylated in MDD patients compared to healthy controls

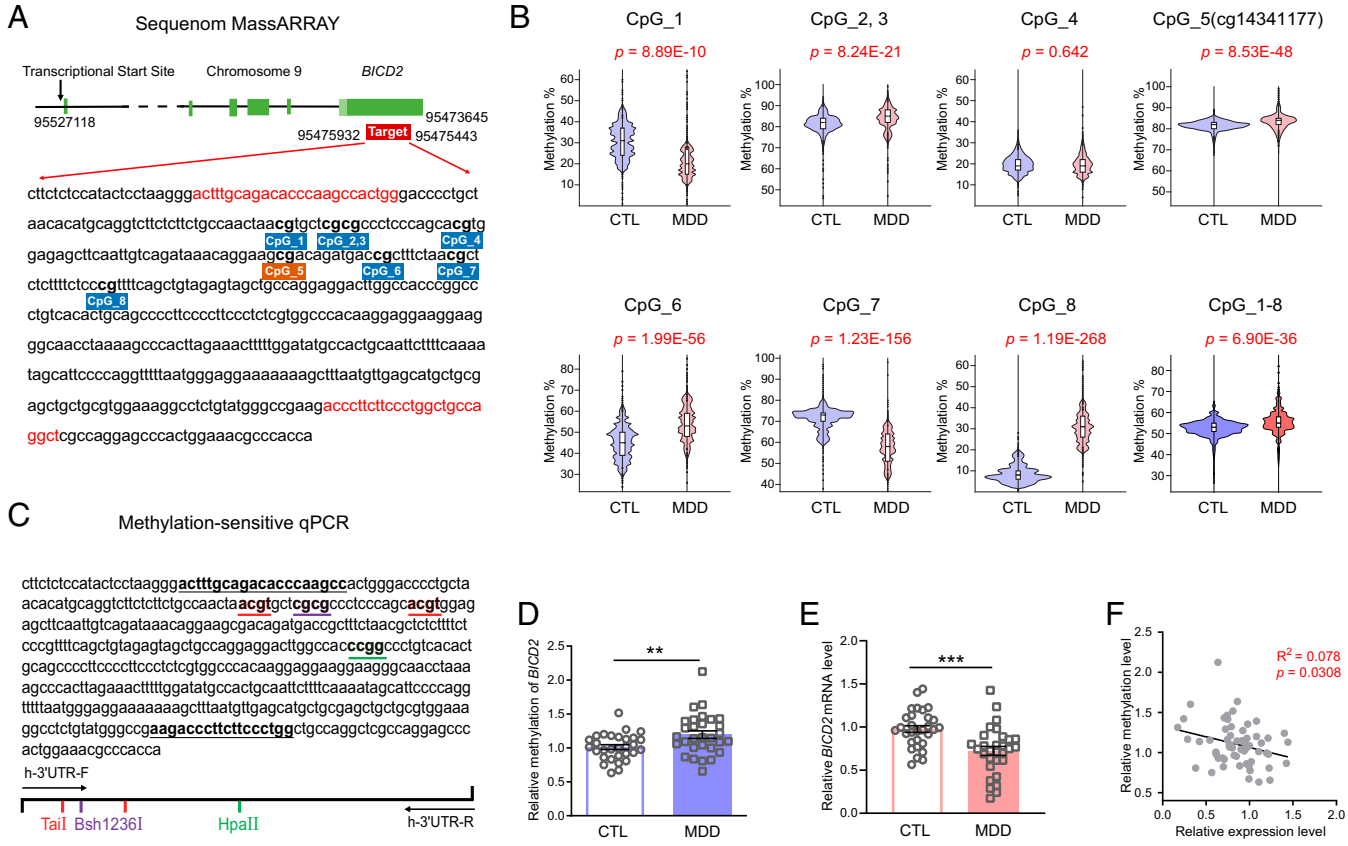

Fig. 2. Replication of the *BICD2*-associated differentially methylated region and its correlation with mRNA expression. (*A*) The CpG sites we detected in the specific region of *BICD2*. (*B*) Violin plot of DNA methylation of CpG sites we detected in MDD patients and healthy controls (CTL). (*C*) The sequence of the specific *BICD2* region assessed by the methylation-sensitive qPCR approach (MSE-qPCR). The primers are underlined, and methylation-sensitive restriction enzymes are represented by different underlines: red for TaiI, purple for Bsh1236I, green for HpaII. (*D*) Relative methylation assessed by MSE-qPCR; $n = 30$ per group. (*E*) qRT-PCR assay for *BICD2* mRNA expression; $n = 30$ per group. (*F*) Correlation analysis of DNA methylation and mRNA expression of *BICD2*; $n = 60$. Data are presented as the mean ± SEM. Unpaired two-tailed Student's *t* test. $^{**}P < 0.01$, $^{***}P < 0.001$.

(P = 8.53E-48), confirming our MWAS result (Fig. 2*B*). The amplicon also contained a CpG site (i.e., CpG_8) corresponding to *cg14184780* on the microarray chip. Although it did not reach the significance threshold for epigenome-wide association studies for *cg14184780* in our DNA methylation microarray analysis ($\Delta\beta$ = 0.02287075; P = 0.03050539), the varying tendency was consistent with CpG_8 in the Sequenom MassArray analysis (P = 1.19E-268). For the other five CpG units, CpG_2, 3 and CpG_6 also showed significant hypermethylation in MDD patients compared to healthy controls, while CpG_1 and CpG_7 demonstrated significant hypomethylation but CpG_4 did not (Fig. 2*B*). We calculated the mean methylation levels in the analysis region by quantifying the average amount of DNA methylation of the seven CpG units (CpG_1-8) and observed significant hypermethylation in MDD patients compared to healthy controls (Fig. 2*B* and Dataset S4). There was no significant gender difference in DNA methylation in the MDD group. In the control group, however, significant gender differences were observed in the CpG_2, 3, CpG_4, CpG_5, CpG_8, and CpG_1-8 sites, indicating that these sites exhibit gender differences only under normal conditions (*SI Appendix*, Table S1). We also performed correlation analysis between DNA methylation of CpG_5 (cg14341177) or CpG1-8 and age and found that there was no significant correlation between DNA methylation and age either in the total population or in each group of the third cohort (*SI Appendix*, Fig. S2). Therefore, although age has considerable effects on DNA methylation, it is not significantly correlated with DNA methylation of *BICD2* in sites analyzed in the current work. These results suggest that methylation analysis of the region chosen may have the potential to discriminate between MDD patients and healthy controls.

Furthermore, we employed the MSE-qPCR approach to quantify DNA methylation and validate the results observed with the Sequenom MassArray method from the fourth cohort of 30 MDD patients and 30 healthy controls (the fourth cohort). It involves the digestion of nonsodium bisulfite-treated genomic DNA using a mixture of methylation-sensitive enzymes followed by qPCR analysis (39). We retrieved four sites within the same region as examined by Sequenom MassArray, which can be cleaved by three methylation-sensitive restriction enzymes (Fig. 2*C*). qPCR analysis revealed significant hypermethylation in MDD patients compared to healthy controls, consistent with the Sequenom MassArray results (Fig. 2*D* and Dataset S5). In addition, the mRNA expression of *BICD2* was significantly lower in the same cohort of MDD patients than healthy controls, confirming the expression microarray results (Fig. 2*E* and Dataset S5). A negative correlation was observed when combined analysis of DNA methylation and mRNA expression of *BICD2* in each subject was performed within the fourth cohort (P = 0.0308, R^2 = 0.078), suggesting a repressive effect of DNA methylation on gene expression (Fig. 2*F* and Dataset S5). There was no significant gender difference in mRNA expression of *BICD2* in either MDD patients or healthy controls of the fourth cohort (*SI Appendix*, Table S2).

Detection of DNA Methylation and mRNA Expression of *Bicd2* in Peripheral Blood and Brain of Mice with Depressive-Like Behaviors. Since we consistently observed increased DNA methylation and decreased mRNA expression of *BICD2* in the peripheral blood of MDD patients, we further conducted a cross-species study in a chronic unpredictable mild stress (CUMS) mouse model of depression (Fig. 3*A*). In the CUMS model, animals experience a series of unpredictable mild stressors within several weeks and ultimately develop depressive-like behaviors, which has been widely used with high validity and translational potential (40). Both the forced swimming test (FST) and sucrose preference test (SPT), which indicate behavioral despair and anhedonia, respectively, showed depressive-like behaviors in CUMS-treated mice (Fig. 3*B* and *C*). We employed the MSE-qPCR approach to determine the DNA methylation in a mouse homologous fragment of the 3′ UTR of *BICD2* that we analyzed in humans. There was 81% similarity between the two fragments from mice and humans. The mouse fragment covers six sites that can be cleaved by methylation-sensitive restriction enzymes (Fig. 3*D*). In the homologous regions, there were four similar CpG sites in human and mouse. Three common CpG sites could be recognized by methylation-sensitive restriction enzymes *Bsh*1236I or *Hpa*II (Figs. 2*C* and 3*D*). For peripheral blood, qPCR analysis revealed significant hypermethylation in CUMS-treated mice compared to control mice, similar to the results in MDD patients (Fig. 3*E* and Dataset S6). The mRNA expression of *Bicd2* was significantly lower in CUMS-treated mice than in control mice (Fig. 3*F* and Dataset S6). Correlation analysis also showed similar results as observed in human studies (P = 0.0131, R^2 = 0.2166), indicating a consistent phenotype between the two species (Fig. 3*G* and Dataset S6).

To investigate the possible functions of BICD2 in MDD, we determined the DNA methylation and mRNA expression of *Bicd2* in major brain regions involved in emotion regulation in mice (41), including the prefrontal cortex, nucleus accumbens, paraventricular nucleus of the hypothalamus, hippocampus, and amygdala (Fig. 3*H*). Interestingly, the MSE-qPCR assay showed significant hypomethylation in the hippocampus of CUMS-treated mice compared to control mice, while the other four brain regions failed to show a difference between the two groups (Fig. 3*I*). At both mRNA and protein levels, CUMS-treated mice demonstrated significantly higher expression in the hippocampus than control mice, suggesting an unrepressed effect of DNA methylation on the gene expression of *Bicd2* (Fig. 3*J* and *K*). BICD2 expression was also significantly increased in the postmortem hippocampus of MDD patients compared with healthy controls, consistent with findings in the mouse model of depression (Fig. 3*L*).

Reduction of Depressive-Like Behaviors in Mice with Hippocampal Knockdown of *Bicd2*. Based on enhanced *Bicd2* expression in the hippocampus of mice with depressive-like behaviors, we employed recombinant adeno-associated virus (rAAV) as a gene transfer vector for in vivo expression of shRNA against *Bicd2*, utilizing shRNA against firefly luciferase as a control (Ctrl) to investigate the function of BICD2 in MDD (Fig. 4*A*). Four weeks after microinjection of rAAV into the bilateral hippocampus (Fig. 4*B*), the BICD2 protein level was significantly decreased in the hippocampus of *Bicd2* shRNA-expressing mice compared to Ctrl shRNA-expressing mice (Fig. 4*C*). After rAAV microinjection, we treated mice with the CUMS procedure to test whether down-regulating the enhanced expression of *Bicd2* in the hippocampus of depressive-like mice exerted antidepressant effects, utilizing fluoxetine administered to CUMS-treated Ctrl shRNA-expressing mice as a therapeutic control (Fig. 4*D*). The immobility duration in the FST was significantly increased in CUMS-treated Ctrl shRNA-expressing mice compared to unstressed Ctrl shRNA-expressing mice, indicating a depression-like consequence induced by CUMS. After CUMS treatment, both *Bicd2* shRNA-expressing mice and fluoxetine-administered Ctrl shRNA-expressing mice showed significantly decreased immobility duration compared to Ctrl

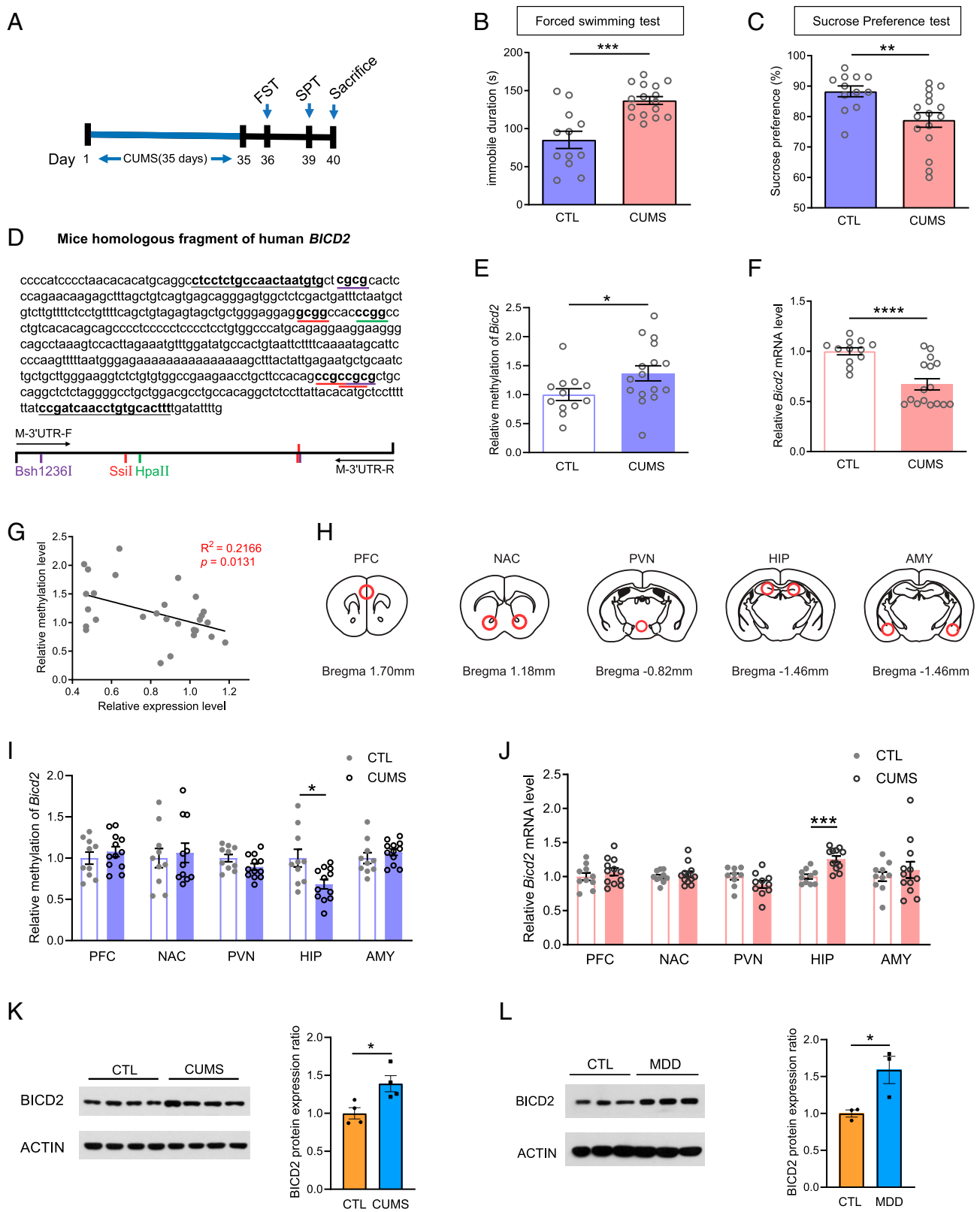

Fig. 3. Detection of DNA methylation and gene expression of *Bicd2* in peripheral blood and brain of mice with depressive-like behaviors, as well as protein expression of postmortem hippocampus of MDD patients. (*A*) Schematic of the CUMS paradigm. FST, forced swimming test; SPT, sucrose preference test. (*B*) Forced swimming test after CUMS. CTL, $n = 12$; CUMS, $n = 16$. (*C*) Sucrose preference test after CUMS. CTL, $n = 12$; CUMS, $n = 16$. (*D*) The homologous fragment of human *BICD2* in mice assessed by MSE-qPCR. The primers are underlined, and methylation-sensitive restriction enzymes are represented by different underlines: red for SsiI, purple for Bsh1236I, green for HpaII. (*E*) Relative methylation of the mouse homologous fragment in the CUMS model assessed by MSE-qPCR. CTL, $n = 12$; CUMS, $n = 16$. (*F*) qRT-PCR assay for *Bicd2* mRNA expression in the peripheral blood of mice. CTL, $n = 12$; CUMS, $n = 16$. (*G*) Correlation analysis of DNA methylation and mRNA expression of *Bicd2*; $n = 28$. (*H*) Schematic diagram shows different brain regions of mice. PFC, prefrontal cortex; NAC, nucleus accumbens; PVN, paraventricular nucleus of the hypothalamus; HIP, hippocampus; and AMY, amygdaloid nucleus. (*I*) Relative methylation of *Bicd2* in various brain regions of CUMS mice assessed by MSE-qPCR; $n = 9$ to 12 mice per group. (*J*) qRT-PCR assay for *Bicd2* mRNA expression in various brain regions of CUMS mice; $n = 9$ to 12 mice per group. (*K*) Western blot assay of BICD2 protein expression in the hippocampus of mice experiencing CUMS. (*L*) Western blot assay of the hippocampus of postmortem human brains. Data are presented as the mean ± SEM. Unpaired two-tailed Student's *t* test. $^{*}P < 0.05$, $^{**}P < 0.01$, $^{***}P < 0.001$, $^{****}P < 0.0001$.

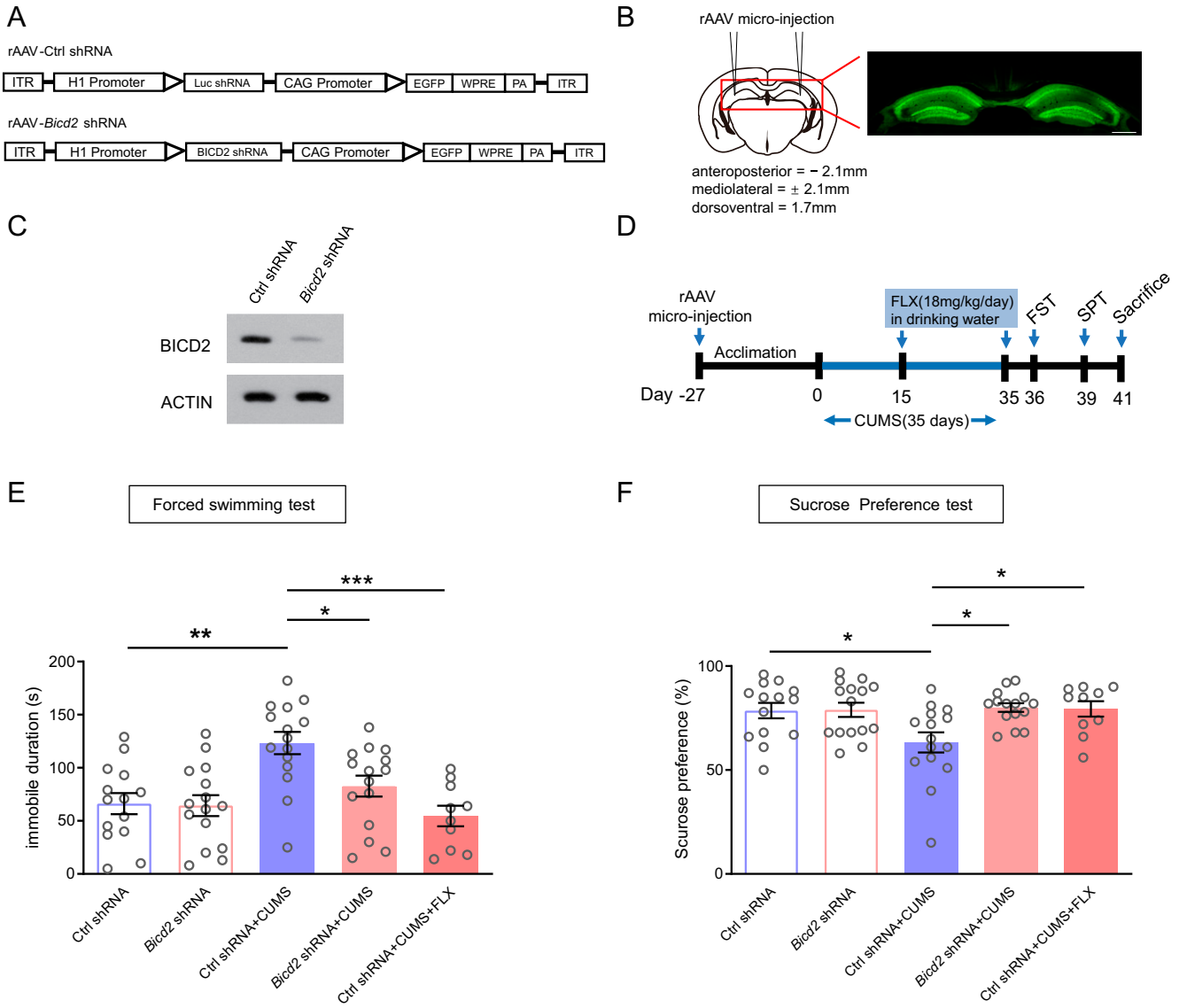

Fig. 4. Reduction of depressive-like behaviors in mice with hippocampal knockdown of *Bicd2*. (*A*) Schematic diagram of the rAAV vectors expressing control (Ctrl) shRNA and *Bicd2* shRNA. (*B*) Validation of *Bicd2* shRNA virus infection into the hippocampus indicated by EGFP fluorescence. (Scale bar, 500 μm.) (*C*) Western blot assay of BICD2 expression in the hippocampus after *Bicd2* shRNA virus microinjection. (*D*) Schematic diagram of the experiment schedule. FLX, fluoxetine. (*E*) Forced swimming test. F = 7.29; n = 10 to 15 per group. (*F*) Sucrose preference test. F = 4.01; n = 10 to 15 per group. Data are presented as the mean ± SEM. One-way ANOVA with Tukey's post hoc analysis. *P < 0.05, **P < 0.01, ***P < 0.001.

shRNA-expressing mice, indicating an antidepressant effect induced by down-regulated expression of *Bicd2* in the hippocampus (Fig. 4*E*). The sucrose preference in the SPT was significantly decreased in CUMS-treated Ctrl shRNA-expressing mice compared to unstressed Ctrl shRNA-expressing mice, confirming the CUMS model of depression. After CUMS treatment, both *Bicd2* shRNA-expressing mice and fluoxetine-administered Ctrl shRNA-expressing mice showed significantly higher sucrose preference than Ctrl shRNA-expressing mice, confirming the antidepressant effect induced by knockdown of *Bicd2* in the hippocampus (Fig. 4*F*). However, there was no significant difference in depressive-like behavior tests between mice with BICD2 overexpression in the hippocampus and control mice, suggesting that BICD2 overexpression in the hippocampus alone is not sufficient to induce depressive-like behaviors (*SI Appendix*, Fig. S3). Whether BICD2 overexpression results in enhanced susceptibility to or impacts the antidepressant effects of therapeutic interventions for depression requires further investigations.

Elevated BDNF Expression Induced by *Bicd2* Knockdown in the Hippocampus or Primary Neurons of Mice. *Bicd2* is reported to regulate subcellular distribution and mRNA local translation of brain-derived neurotrophic factor (BDNF), a key molecule intimately involved in the pathophysiology and treatment response of depression (42, 43). Either single infusion or virus-mediated overexpression of BDNF in the hippocampus exerts antidepressant effects in rat models of depression (44, 45). Although loss of hippocampal BDNF does not sufficiently induce depressive-like behavior, selective knockout of *Bdnf* in the dentate gyrus attenuates antidepressant efficacy (46). Therefore, we sought to examine whether knockdown of *Bicd2* affects the expression and function of BDNF. There was no difference in the mRNA expression of *Bdnf* in the hippocampus between *Bicd2* knockdown and control mice; however, the hippocampal BDNF protein level was significantly up-regulated in *Bicd2* shRNA-expressing mice compared to control mice (Fig. 5*A*–*C*). Tropomyosin-related kinase B (TrkB), the major

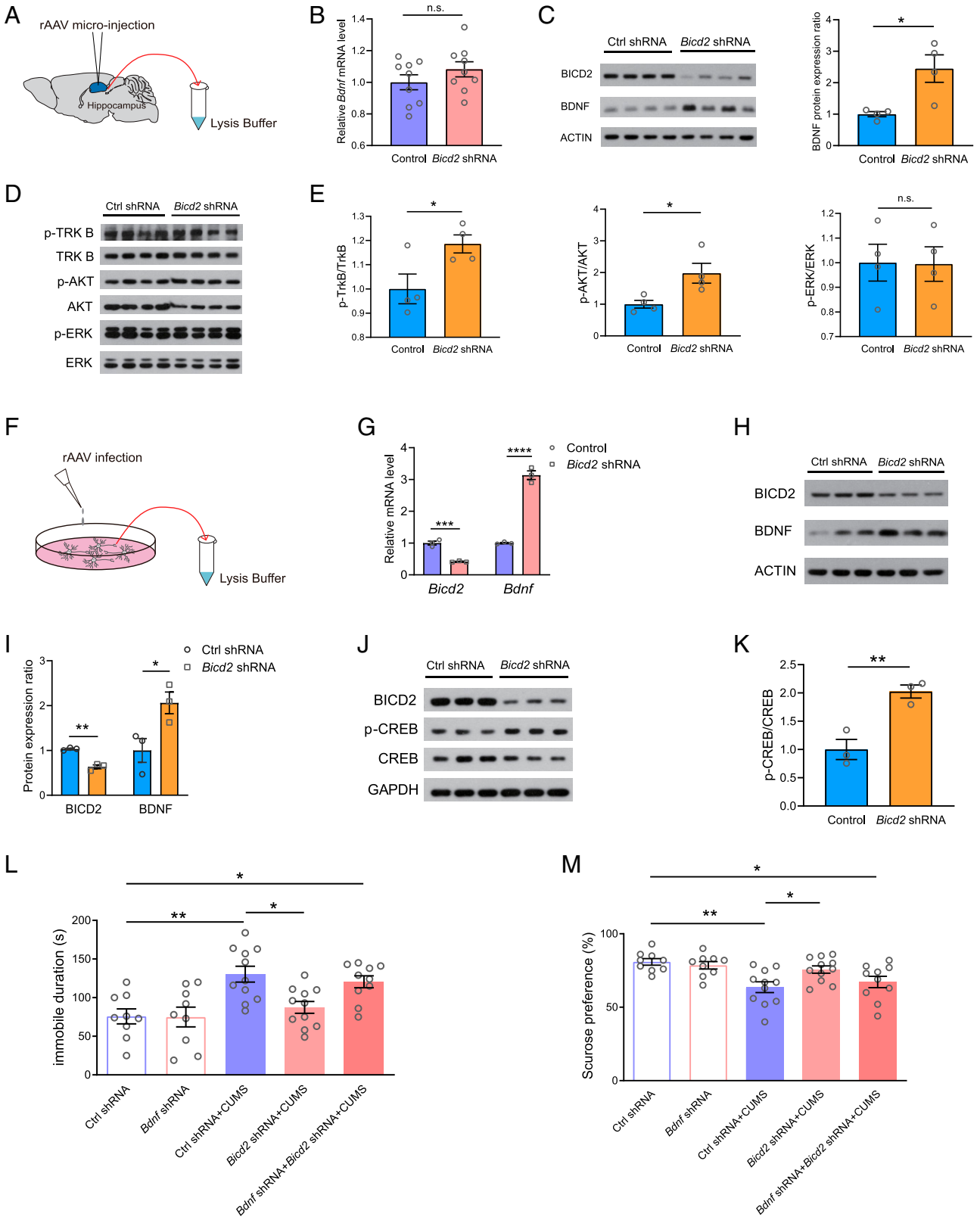

Fig. 5. Elevated BDNF expression induced by *Bicd2* knockdown mediated the antidepressant effects of BICD2 down-regulation in the hippocampus of mice. (*A*) Schematic of hippocampal tissue protein extraction after virus microinjection. (*B*) qPCR assay for *Bdnf* mRNA expression in the hippocampus microinjected with *Bicd2* shRNA- or Ctrl shRNA-expressing rAAVs; $n = 9$ per group. (*C–E*) Western assay for protein expressions of BICD2, BDNF, p-TRKB, p-AKT; and p-ERK in the hippocampus of mice injected with *Bicd2* shRNA- or Ctrl shRNA-expressing rAAVs. (*F*) Schematic of primary hippocampal neuron protein extraction after virus injection. (*G*) qPCR assay for *Bicd2* and *Bdnf* mRNA expressions in primary hippocampal neurons infected with *Bicd2* shRNA- or Ctrl shRNA-expressing rAAVs. (*H–K*) Western assay for protein expressions of BICD2, BDNF, and p-CREB in primary hippocampal neurons infected with *Bicd2* shRNA- or Ctrl shRNA-expressing rAAVs. (*L*) Forced swimming test. $F = 7.24$; $n = 9$ to 11 per group. (*M*) Sucrose preference test. $F = 5.77$; $n = 9$ to 11 per group. Data are presented as the mean ± SEM. One-way ANOVA with Tukey's post hoc analysis for *L* and *M* and unpaired two-tailed Student's *t* test for other statistics. $^{*}P < 0.05$, $^{**}P < 0.01$, $^{***}P < 0.001$, $^{****}P < 0.0001$. n.s., not significant.

high-affinity receptor for BDNF, was more phosphorylated in the *Bicd2* knockdown hippocampus than the control hippocampus, indicating activated BDNF signaling pathways (Fig. 5*D* and *E*). For the main downstream signaling molecules, we detected more phosphorylated protein kinase B (pAkt) in the *Bicd2* shRNA-expressing hippocampus than the control but failed to find a difference in phosphorylated extracellular signal-regulated protein kinase (pERK) between the two groups, suggesting that BDNF/TrkB/Akt may be involved in the antidepressant effects of hippocampal knockdown of *Bicd2* (Fig. 5*D* and *E*). Owing to the cellular heterogeneity in the hippocampus, we further examined the influence of *Bicd2* knockdown on the expression of *Bdnf* in primary mouse hippocampal neurons (Fig. 5*F*). Both the mRNA and protein expression levels of *Bdnf* were significantly elevated in *Bicd2* shRNA-expressing neurons compared to control neurons, suggesting that *Bicd2* knockdown may affect *Bdnf* transcription and/or mRNA stability (Fig. 5*G*–*I* and *SI Appendix*, Fig. S4). Upstream of the BDNF signaling pathways, we found that *Bicd2* knockdown markedly increased the phosphorylation of cAMP-response element binding protein (CREB) in cultured hippocampal neurons (Fig. 5*J* and *K*), which is the classic transcription factor regulating *Bdnf* transcription (47, 48). When mice were coinfected with AAV-*Bicd2* shRNA and AAV-*Bdnf* shRNA in the hippocampus, they still exhibited depressive-like behaviors after the CUMS treatment, indicating that *Bdnf* down-regulation blocks the antidepressant effects of *Bicd2* knockdown in the hippocampus of mice (Fig. 5*L* and *M* and *SI Appendix*, Fig. S5). The above results suggest that increased BDNF expression may mediate the antidepressant effects of hippocampal *Bicd2* knockdown.

Discussion

Here, we report DNA hypermethylation and mRNA down-regulation of the *BICD2* gene in the peripheral blood of MDD patients by employing multiple detection methods in four independent cohorts. The results were replicated in the peripheral blood of mice with depressive-like behaviors, while *Bicd2* in the hippocampus showed DNA hypomethylation and mRNA/protein up-regulation. BICD2 protein was also up-regulated in the postmortem hippocampus of MDD patients. Hippocampal *Bicd2* knockdown demonstrates antidepressant action in the CUMS mouse model of depression, which may be mediated by increased BDNF expression. Our study identified and validated a potential DNA methylation biomarker; its functional implications would be exploited to improve the diagnosis and treatment of MDD (*SI Appendix*, Fig. S6).

By stringent criteria (absolute delta beta [Δβ] value >0.2 and *P* value $<3.6 \times 10^{-8}$ for MWAS; absolute Log_2 fold change >1 and *P* value <0.01 for RNA microarray), we identified three genes (*BICD2*, *RABGGTB*, and *CDKN1C*) that demonstrated DNA hypermethylation and mRNA down-regulation in the peripheral blood of individuals with MDD. *RABGGTB*, encoding the Rab geranylgeranyl transferase beta (RabGGTase beta) catalytic subunit, has not been widely investigated (49). One recent study reported decreased RABGGTB protein expression in the postmortem dorsolateral prefrontal cortex from patients with schizophrenia (50); however, its function needs further investigation. *CDKN1C*, also known as p57KIP2 encoding cyclin-dependent kinase inhibitor 1C, is a putative tumor suppressor gene that negatively regulates cell proliferation (51) and is involved in cerebral cortex development (52). Whether *CDKN1C* can serve as a potential biomarker for and play a role in MDD also needs further investigation. BICD2 is a motor activating adaptor protein structurally consisting of three coiled-coil (CC) domains. The N-terminal CC1 domain interacts with the dynein–dynactin complex, the CC2 domain interacts with KIF5A, and the C-terminal CC3 domain binds to cargo proteins, such as RAB6A and RANBP2 (53). It induces selective dynein-mediated microtubule minus end-directed transport (29), regulating the positioning of several organelles, such as the nucleus and centrosomes (30, 32) and the endoplasmic reticulum exit sites around the Golgi (31). Recent studies have revealed that BICD2 is required for neuronal migration (33–36), indicating its fundamental role in neural development. Although multiple mutations in *BICD2* have been reported to be associated with spinal muscular atrophy (37), the current work reports the association of *BICD2* DNA methylation with MDD and the functional consequences of its altered expression in an animal model of depression.

In this study, the *cg14341177* site identified with the HM450 assay in individuals with MDD was not reported by previous MWAS (13–22), which may be due to the relatively low reproducibility of the genes identified by each MWAS, implying that multiple factors can affect the dynamic changes of DNA methylation. In addition, we combined transcriptome analysis to screen potential biomarkers for MDD, which may also exert a role in the pathophysiology of MDD. Validation studies in two independent cohorts confirmed the hypermethylated changes in *BICD2* in the blood of individuals with MDD, and cross-species studies in a mouse model of depression further supported our findings. These results make us so confident that the DNA methylation level of *BICD2* is associated with MDD. Among the 55 genes identified with the HM450 assay, *TOX2* (TOX high mobility group box family member 2) has recently been reported to be associated with MDD in a genome-wide regional heritability mapping study (54). The *cg15403961* site in the *GALNTL6* gene was significantly hypomethylated in MDD patients in our study, which reveals the same direction change as *cg18329797*, another site in GALNTL6 reported by other investigators (17). Similarly, the *cg06662428* site in the PAOX gene was identified in our study ($\Delta\beta = -0.28527725$; $P = 5.68\text{E-}39$), while another site (*cg11975206*) in the same gene was reported in an MWAS of peripheral leukocytes from medication-free patients with MDD (14). These results indicate that different sites on the same gene may be epigenetically modified under different conditions in MDD. Previous studies with a candidate gene strategy have reported changes in the DNA methylation of several genes associated with MDD, such as *BDNF*, *SLC6A4*, *OXTR*, and *FKBP5* (12). However, for probes targeting those genes, the absolute Δβ was less than 0.2 in our study, although some sites reached a *P* value $<3.6 \times 10^{-8}$, suggesting that they may not be suitable to serve as biomarkers (Dataset S7).

DNA methylation possesses a tissue- and cell type–specific nature (55). An important question in biomarker identification for psychiatric disorders is the correspondence between blood and brain tissue. Previous studies have shown a moderate correlation between blood and brain tissue by genome-wide DNA methylation comparison (56–59). A recent study reported a significant overlap between the top MWAS findings in blood and Brodmann area 10, but not Brodmann area 25 of the brain (19). In contrast to the findings in blood, CUMS treatment intriguingly decreased DNA methylation and increased mRNA expression of *Bicd2* in the hippocampus of mice, while there was no change in other examined regions regulating emotions, suggesting that the hippocampus is the main area where *Bicd2* contributes to the pathophysiology of depression. The mechanisms underlying the differential methylation changes between

blood and brain remain to be explored. However, such a case appears to be common (60–63). For the mechanisms, several points may be considered. First, we conducted bulk analysis of DNA methylation in whole blood and the hippocampus in this study. White blood cells (WBCs) in the whole blood consist of a number of distinct cell types, including granulocytes, lymphocytes, and monocytes, each of which can be further divided into subpopulations. In recent years, an increasing interest in the immune mechanisms contributing to the pathogenesis of MDD has been documented (64) and immunological therapeutic targets for depression have been developed (65). The number and proportion of different blood cell types are altered in depressed patients, which can be employed to distinguish subgroups of depression (66). Therefore, MWAS analysis of single cell or cell type may provide an insight into the DNA methylation changes in blood of MDD patients. A similar strategy should be applied to the brain that also contains various cell types such as neurons, astrocytes, microglia, oligodendrocytes, endothelial cells, and pericytes, exhibiting differential DNA methylations (67). Second, the brain is a complex organ with numerous subregions interconnected and coordinated to regulate behaviors. Different brain regions do not necessarily make consistent changes in DNA methylation and gene expression in response to the same stimuli. Indeed, opposite changes in DNA methylation were observed between the cerebellum and putamen of patients with Parkinson's disease (68). Low serum BDNF concentrations were reported in antidepressant-free depressed patients relative to healthy controls and to antidepressant-treated depressed patients (69). However, in the brain, the role of BDNF in depression depends on its location in the neural circuitry. In rodent models of depression, expression of BDNF is decreased in the hippocampus and prefrontal cortex, but increased in the nucleus accumbens and amygdala (70). Similarly, the role of BICD2 in depression is inextricably linked with its location in the neural circuitry. Third, the complicated interactions between peripheral tissues such as blood cells and the central nervous system pose a big challenge to determine the cause-and-effect of DNA methylation changes in the pathophysiology of depression. Functional studies by manipulating the methylation levels of the identified sites could help to clarify this issue. Overall, although we have not pinpointed the cause of the opposite findings in DNA methylation and gene expression of *Bicd2* in the hippocampus versus whole blood of mice with depressive-like behaviors, this does not prevent it from being a potential biomarker of depression.

We also found that reducing the increased expression of *Bicd2* in the hippocampus exerts antidepressant effects in CUMS-treated mice, which is accompanied by up-regulated BDNF expression. Further analysis showed that hippocampal knockdown of *Bicd2* activates the BDNF/TrkB/Akt pathway in vivo and promotes BDNF transcription by activating CREB in cultured primary neurons. These results suggest that the BDNF signaling pathway is likely to underlie the antidepressant effects of *Bicd2* knockdown in the hippocampus of mice with depressive-like behaviors. Indeed, it has been reported that BICD2 regulates the subcellular distribution and mRNA local translation of BDNF (42). BICD1, one of the two isoforms of BICD proteins in mammals that can partially compensate for BICD2's function (71), regulates the intracellular sorting of BDNF receptors, and depleting BICD1 results in more sustained AKT activation in response to BDNF stimulation (72). BDNF expression is reduced in the hippocampus of MDD patients (43), while elevating BDNF levels in the hippocampus exerts antidepressant effects in animal models of depression (44, 45). Therefore, *Bicd2* knockdown-induced up-regulation of BDNF in the hippocampus may contribute to the observed antidepressant phenotypes.

There are several limitations to our study. First, although HM450 is an economic and efficient high throughput assay for MWAS, the coverage is still far from complete in light of all 28 million common CpG sites in the human genome. Thus, using a sequencing-based approach may uncover more significant sites. Second, it is important to note that the cross-sectional design of the study cannot confirm whether changes in DNA methylation of *BICD2* may predict the response to antidepressant treatment and serve as a prognostic biomarker. Therefore, a longitudinal study is needed in future work. Third, whether altered *BICD2* DNA methylation also occurs in other psychiatric disorders, such as anxiety, posttraumatic stress disorder, and schizophrenia, warrants further study. Fourth, only male mice were employed in this study. Given the higher incidence of depression in women, further work on the role of BICD2 in female mice may corroborate to demonstrate its changes and functions in depression. Finally, the molecular and cellular mechanisms by which BICD2 may play a role in the pathogenesis of depression remain to be further investigated, especially in regulating the BDNF signaling pathway.

In summary, our findings suggest that the *BICD2* DNA methylation test may assist in the diagnosis of MDD and that hippocampal BICD2 plays a role in the pathophysiology of MDD. However, causal data are lacking to illustrate whether manipulating the methylation levels of the identified sites could affect the development and treatment of MDD. By cutting-edge gene editing techniques (73), future studies may achieve site-specific mutations in vivo to examine the roles of the targeted DNA methylation sites in developing depression.

Materials and Methods

Human Subjects and Animals. Healthy controls and MDD patients all gave written informed consent to attend this study. The study was approved by the Ethics Committee of the Chinese Academy of Medical Sciences and the Peking Union Medical College. Hippocampal tissues of the human brain were provided by the National Human Brain Bank for Development and Function, Chinese Academy of Medical Sciences, and Peking Union Medical College, Beijing, China (*SI Appendix*, Table S3). The protocol number is 2019017. The donation of human tissue was voluntary and free, approved by the donor and all the donor's direct family members. It was also approved that the donated human tissue will only be used for scientific research.

All the subjects recruited for this study were of Chinese Han origin and geographically came from northern China. In 2011 to 2021, we recruited 1,526 subjects, including 908 healthy controls (389 men and 519 women) aged 36.5 ± 14.3, and 618 patients with MDD (256 men and 362 women) aged 36.7 ± 13.2 through the Department of Psychiatry, First Hospital of Shanxi Medical University, Taiyuan, China. None of the cohorts has been reported elsewhere. The demographic information of each cohort is detailed in *SI Appendix*, Table S4. There was no significant difference in the gender distribution of each cohort by Pearson's chi-square test (*SI Appendix*, Table S5). The first cohort and second cohort were generated as "discovery/study cohorts" for genome-wide DNA methylation and transcriptome profiling. In order to ensure the homogeneity of MDD patients, only drug-naïve inpatients in acute episode were included. Moreover, these patients all underwent clinical visits for more than a year and did not have any anxiety symptoms, ruling out the interference of bipolar disorder. The third cohort was an "expanded validation cohort" for validating targeted DNA methylation sites, which was to determine whether the methylation level of cg14341177 identified by the first two cohorts was significantly elevated in a larger population of MDD patients. MDD patients in this cohort were all in acute depressive episodes, and the patients self-reported their first depressive episode at least 6 mo ago, with no manic manifestations during this period (so that we

excluded the possibility of bipolar disorder), no history of psychiatric or psychological visits, and no recent use of antidepressant medications. The fourth cohort was an "independent validation cohort" for the first two cohorts with consistent inclusion criteria, which was to determine the changes in DNA methylation and mRNA expression of *BICD2* with alternative approaches and directly observe the negative correlation between DNA methylation and mRNA expression of *BICD2* from the same subjects. All patients were assessed by at least two consultant psychiatrists according to the Diagnostic and Statistical Manual of Mental Disorders Fourth Edition (DSM- IV) and the 17-item Hamilton rating scale for depression (HAMD-17) criteria for MDD. None of the MDD patients or healthy controls had taken any psychotropic medications within 4 wk prior to the recruitment of study.

The sample sizes for the first, second, and fourth cohorts were determined according to the criterion that the global false discovery rate (FDR) was less than 5%. The sample size for the third cohort was calculated using the G*Power 3.1 software. The calculation parameters are as follows: 1) effect size = 0.2; 2) α = 0.05; 3) power = 0.9; 4) numerator df = 3 (group, sex, and age); 5) number of groups = 2; and 6) number of covariates = 2 (sex and age). By these calculation parameters, G*Power 3.1 suggested that the minimum of 359 participants was needed for each group (n = 718) in a one-way ANOVA test.

Animals. All animal studies were approved by the Institute of Basic Medical Sciences, Chinese Academy of Medical Sciences Institutional Review Board. Adult male C57BL/6J mice aged 8 wk were purchased from Vital River Laboratories. Mice were acclimatized for 1 wk before the experiment in a temperature of 23 °C ± 2 °C and humidity of 60% ± 5% as well as a controlled environment with a 12-h dark/12-h light cycle with free access to food and water.

Genome-Wide DNA Methylation Profiling Using an Illumina Microarray. Forty healthy controls and 40 MDD patients who had never been treated with depression medication were enrolled for genome-wide DNA methylation detection. Genome-wide DNA methylation was performed using an Illumina Infinium Human Methylation 450 K bead chip that obtained the methylation profile of each sample at over 485,000 CpG sites. The genomic DNA was bisulfite converted using the EZ-96 DNA Methylation-Gold Kit (D5008, Zymo Research). Bisulfite-converted DNA hybridization and labeling were performed according to the manufacturer's protocol for the Illumina 450 K array. The raw intensity was extracted using Genome Studio software. The sites with detection P values >0.05 were not reliable and were excluded from further analysis. DNA methylation data were normalized using the R minfi package (74). Differential methylation analysis between groups was performed using the ChAMP package (75). P values were adjusted for multiple testing using the Benjamini–Hochberg procedure (76). Differentially methylated positions (DMPs) were extracted using a threshold of adjusted P value $<3.6 \times 10^{-8}$ and absolute value of delta beta >0.2.

Human Gene Expression Microarray. The quality of total blood RNA was confirmed with an Agilent 2100 (Agilent Technologies). In brief, double-stranded cDNAs were synthesized from total RNA using reverse transcriptase, and the double-stranded cDNAs were then transcribed into cRNA in vitro. The cRNA was fluorescently labeled and hybridized using a 4 × 180 K lncRNA+mRNA Human Gene Expression Microarray V3.0 (CapitalBio, Technology) to detect genome-wide gene expression. Agilent Feature Extraction software was applied to extract the data. The array data were analyzed for data summarization, normalization, and quality control by using GeneSpring software (Agilent). A t test was applied to analyze sample data of two groups to obtain the Benjamini–Hochberg corrected P values and fold change values.

Sequenom MassARRAY Methylation Analysis. The Sequenom MassARRAY platform (BioMiao Biological Technology) was used to quantitatively examine methylation according to the protocol recommended by the manufacturer (38). The genomic DNA was bisulfite-converted using the EZ-96 DNA Methylation-Gold Kit (D5008, Zymo Research). The primers were designed by EpiDesigner software (www.epidesigner.com). The sequences of the primers of the target sequence were 5′-aggaagagagAGTTTGGTAGTTAGGGAAGAAGGGT-3′ (forward primer) and 5′-cagtaatacgactcactatagggagaaggctACTTTACAAACACCCAAACCACTAA-3′ (reverse primer). The T7 promoter sequence was added to the PCR products, and in vitro RNA transcription was then performed and processed by base-specific cleavage. Small RNA fragments with CpG sites were obtained. The time of flight mass spectrometry (MALDI-TOF MS) was used to determine the molecular weights of each fragment. The methylation level of individual units was measured by quantitative methylation analysis (Sequenom). A linear regression model was used on the Sequenom MassARRAY methylation data to analyze the differences in methylation levels between groups (MDD and control) with adjustment for sex (male and female) and age.

The following experiments and analyses are described in *SI Appendix, SI Materials and Methods*, including DNA and RNA extraction, *BICD2* 3′ UTR methylation by MSR-qPCR, qRT-PCR, Western blot, vector construction, rAAV packaging and microinjection, antidepressant administration, CUMS procedure, behavioral tests, forced swimming test, sucrose preference test, primary hippocampus neuron culture and rAAV infection, and statistical analysis.

Data Availability. The 450 K methylation microarray data generated in this study have been deposited in the Gene Expression Omnibus (GEO) database under accession code GSE201287 (https://www.ncbi.nlm.nih.gov/geo/query/acc.cgi?acc=GSE201287) (77). The transcriptome profiling data have been deposited in the GEO database under accession code GSE201332 (https://www.ncbi.nlm.nih.gov/geo/query/acc.cgi?acc=GSE201332) (78). All other study data are included in the article and/or supporting information.

ACKNOWLEDGMENTS. This work was supported by research grants from the Ministry of Science and Technology of the People's Republic of China (2021ZD0203001 to Q.X., 2022ZD0211700 to J.X., 2021ZD0200600 to H.W., and 2021ZD0202001 to C.Z.), the National Key Research and Development Program of China (2020YFA0804502 to Q.X.), the National Natural Science Foundation of China (81930104 to Q.X., 31970952 to J.X., and 82101545 to W.Z.), Chinese Academy of Medical Sciences (CAMS) Innovation Fund for Medical Sciences (2021- I2M- 1-020 to Q.X.), and the Science and Technology Program of Guangdong (2018B030334001 to Q.X.). We thank the Institute of Basic Medical Sciences, CAMS, Neuroscience Center, and the China Human Brain Banking Consortium for providing the hippocampal tissues of the human brain.

1. M. J. Friedrich, Depression is the leading cause of disability around the world. *JAMA* **317**, 1517 (2017).
2. R. C. Kessler, E. J. Bromet, The epidemiology of depression across cultures. *Annu. Rev. Public Health* **34**, 119–138 (2013).
3. R. Mayeux, Biomarkers: Potential uses and limitations. *NeuroRx* **1**, 182–188 (2004).
4. J. Mill, A. Petronis, Molecular studies of major depressive disorder: The epigenetic perspective. *Mol. Psychiatry* **12**, 799–814 (2007).
5. P. F. Sullivan, M. C. Neale, K. S. Kendler, Genetic epidemiology of major depression: Review and meta-analysis. *Am. J. Psychiatry* **157**, 1552–1562 (2000).
6. CONVERGE consortium, Sparse whole-genome sequencing identifies two loci for major depressive disorder. *Nature* **523**, 588–591 (2015).
7. N. R. Wray *et al.*; eQTLGen; 23andMe; Major Depressive Disorder Working Group of the Psychiatric Genomics Consortium, Genome-wide association analyses identify 44 risk variants and refine the genetic architecture of major depression. *Nat. Genet.* **50**, 668–681 (2018).
8. D. M. Howard *et al.*; 23andMe Research Team; Major Depressive Disorder Working Group of the Psychiatric Genomics Consortium, Genome-wide meta-analysis of depression identifies 102 independent variants and highlights the importance of the prefrontal brain regions. *Nat. Neurosci.* **22**, 343–352 (2019).
9. T. Klengel, E. B. Binder, Epigenetics of stress-related psychiatric disorders and gene × environment interactions. *Neuron* **86**, 1343–1357 (2015).
10. R. Holliday, J. E. Pugh, DNA modification mechanisms and gene activity during development. *Science* **187**, 226–232 (1975).
11. G. Cai *et al.*; ColonAiQ Group, A multilocus blood-based assay targeting circulating tumor DNA methylation enables early detection and early relapse prediction of colorectal cancer. *Gastroenterology* **161**, 2053–2056.e2 (2021).
12. M. Li *et al.*, What do DNA methylation studies tell us about depression? A systematic review. *Transl. Psychiatry* **9**, 68 (2019).
13. J. Guintivano, M. Arad, T. D. Gould, J. L. Payne, Z. A. Kaminsky, Antenatal prediction of postpartum depression with blood DNA methylation biomarkers. *Mol. Psychiatry* **19**, 560–567 (2014).
14. S. Numata *et al.*, Blood diagnostic biomarkers for major depressive disorder using multiplex DNA methylation profiles: Discovery and validation. *Epigenetics* **10**, 135–141 (2015).
15. A. Córdova-Palomera *et al.*, Genome-wide methylation study on depression: Differential methylation and variable methylation in monozygotic twins. *Transl. Psychiatry* **5**, e557 (2015).
16. M. Shimada *et al.*, An epigenome-wide methylation study of healthy individuals with or without depressive symptoms. *J. Hum. Genet.* **63**, 319–326 (2018).
17. B. Crawford *et al.*; Major Depressive Disorder Working Group of the Psychiatric Genomics Consortium, DNA methylation and inflammation marker profiles associated with a history of depression. *Hum. Mol. Genet.* **27**, 2840–2850 (2018).
18. O. Story Jovanova *et al.*, DNA methylation signatures of depressive symptoms in middle-aged and elderly persons: Meta-analysis of multiethnic epigenome-wide studies. *JAMA Psychiatry* **75**, 949–959 (2018).
19. K. A. Aberg *et al.*, Methylome-wide association findings for major depressive disorder overlap in blood and brain and replicate in independent brain samples. *Mol. Psychiatry* **25**, 1344–1354 (2020).

20. W. Wang *et al.*, Genome-wide DNA methylation and gene expression analyses in monozygotic twins identify potential biomarkers of depression. *Transl. Psychiatry* **11**, 416 (2021).
21. D. M. Howard *et al.*, Methylome-wide association study of early life stressors and adult mental health. *Hum. Mol. Genet.* **31**, 651–664 (2022).
22. M. N. Davies *et al.*; UK Brain Expression Consortium, Hypermethylation in the ZBTB20 gene is associated with major depressive disorder. *Genome Biol.* **15**, R56 (2014).
23. C. Ju *et al.*, Integrated genome-wide methylation and expression analyses reveal functional predictors of response to antidepressants. *Transl. Psychiatry* **9**, 254 (2019).
24. L. Sirignano *et al.*, Methylome-wide change associated with response to electroconvulsive therapy in depressed patients. *Transl. Psychiatry* **11**, 347 (2021).
25. J. Yu *et al.*, DNA methyltransferases: Emerging targets for the discovery of inhibitors as potent anticancer drugs. *Drug Discov. Today* **24**, 2323–2331 (2019).
26. Q. LaPlant *et al.*, Dnmt3a regulates emotional behavior and spine plasticity in the nucleus accumbens. *Nat. Neurosci.* **13**, 1137–1143 (2010).
27. N. C. Gassen *et al.*, Chaperoning epigenetics: FKBP51 decreases the activity of DNMT1 and mediates epigenetic effects of the antidepressant paroxetine. *Sci. Signal.* **8**, ra119 (2015).
28. A. Saffari *et al.*, Estimation of a significance threshold for epigenome-wide association studies. *Genet. Epidemiol.* **42**, 20–33 (2018).
29. C. C. Hoogenraad *et al.*, Bicaudal D induces selective dynein-mediated microtubule minus end-directed transport. *EMBO J.* **22**, 6004–6015 (2003).
30. D. J. Hu *et al.*, Dynein recruitment to nuclear pores activates apical nuclear migration and mitotic entry in brain progenitor cells. *Cell* **154**, 1300–1313 (2013).
31. O. Shomron *et al.*, Positioning of endoplasmic reticulum exit sites around the Golgi depends on BicaudalD2 and Rab6 activity. *Traffic* **22**, 64–77 (2021).
32. D. Splinter *et al.*, Bicaudal D2, dynein, and kinesin-1 associate with nuclear pore complexes and regulate centrosome and nuclear positioning during mitotic entry. *PLoS Biol.* **8**, e1000350 (2010).
33. D. Jaarsma *et al.*, A role for Bicaudal-D2 in radial cerebellar granule cell migration. *Nat. Commun.* **5**, 3411 (2014).
34. L. Will *et al.*, Dynein activating adaptor BICD2 controls radial migration of upper-layer cortical neurons in vivo. *Acta Neuropathol. Commun.* **7**, 162 (2019).
35. M. H. Tsai *et al.*, Impairment in dynein-mediated nuclear translocation by BICD2 C-terminal truncation leads to neuronal migration defect and human brain malformation. *Acta Neuropathol. Commun.* **8**, 106 (2020).
36. J. C. Gonçalves, S. Quintremil, J. Yi, R. B. Vallee, Nesprin-2 recruitment of BicD2 to the nuclear envelope controls dynein/kinesin-mediated neuronal migration in vivo. *Curr. Biol.* **30**, 3116–3129.e4 (2020).
37. D. C. Koboldt, M. A. Waldrop, R. K. Wilson, K. M. Flanigan, The genotypic and phenotypic spectrum of BICD2 variants in spinal muscular atrophy. *Ann. Neurol.* **87**, 487–496 (2020).
38. M. Ehrich *et al.*, Quantitative high-throughput analysis of DNA methylation patterns by base-specific cleavage and mass spectrometry. *Proc. Natl. Acad. Sci. U.S.A.* **102**, 15785–15790 (2005).
39. K. Hashimoto, S. Kokubun, E. Itoi, H. I. Roach, Improved quantification of DNA methylation using methylation-sensitive restriction enzymes and real-time PCR. *Epigenetics* **2**, 86–91 (2007).
40. P. Willner, The chronic mild stress (CMS) model of depression: History, evaluation and usage. *Neurobiol. Stress* **6**, 78–93 (2016).
41. J. Muir, J. Lopez, R. C. Bagot, Wiring the depressed brain: Optogenetic and chemogenetic circuit interrogation in animal models of depression. *Neuropsychopharmacology* **44**, 1013–1026 (2019).
42. S. Oe, H. Miki, W. Nishimura, Y. Noda, Mechanism of the dendritic translation and localization of brain-derived neurotrophic factor. *Cell Struct. Funct.* **41**, 23–31 (2016).
43. E. Castrén, L. M. Monteggia, Brain-derived neurotrophic factor signaling in depression and antidepressant action. *Biol. Psychiatry* **90**, 128–136 (2021).
44. Y. Shirayama, A. C. Chen, S. Nakagawa, D. S. Russell, R. S. Duman, Brain-derived neurotrophic factor produces antidepressant effects in behavioral models of depression. *J. Neurosci.* **22**, 3251–3261 (2002).
45. D. Taliaz *et al.*, Resilience to chronic stress is mediated by hippocampal brain-derived neurotrophic factor. *J. Neurosci.* **31**, 4475–4483 (2011).
46. M. Adachi, M. Barrot, A. E. Autry, D. Theobald, L. M. Monteggia, Selective loss of brain-derived neurotrophic factor in the dentate gyrus attenuates antidepressant efficacy. *Biol. Psychiatry* **63**, 642–649 (2008).
47. P. B. Shieh, S. C. Hu, K. Bobb, T. Timmusk, A. Ghosh, Identification of a signaling pathway involved in calcium regulation of BDNF expression. *Neuron* **20**, 727–740 (1998).
48. X. Tao, S. Finkbeiner, D. B. Arnold, A. J. Shaywitz, M. E. Greenberg, Ca2+ influx regulates BDNF transcription by a CREB family transcription factor-dependent mechanism. *Neuron* **20**, 709–726 (1998).
49. C. Chinpaisal, C. H. Lee, L. N. Wei, Studies of the mouse Rab geranylgeranyl transferase beta subunit: Gene structure, expression and regulation. *Gene* **184**, 237–243 (1997).
50. A. L. Pinner, T. M. Mueller, K. Alganem, R. McCullumsmith, J. H. Meador-Woodruff, Protein expression of prenyltransferase subunits in postmortem schizophrenia dorsolateral prefrontal cortex. *Transl. Psychiatry* **10**, 3 (2020).
51. S. Matsuoka *et al.*, p57KIP2, a structurally distinct member of the p21CIP1 Cdk inhibitor family, is a candidate tumor suppressor gene. *Genes Dev.* **9**, 650–662 (1995).
52. S. Laukoter *et al.*, Imprinted Cdkn1c genomic locus cell-autonomously promotes cell survival in cerebral cortex development. *Nat. Commun.* **11**, 195 (2020).
53. L. A. Martinez-Carrera, B. Wirth, Dominant spinal muscular atrophy is caused by mutations in BICD2, an important golgin protein. *Front. Neurosci.* **9**, 401 (2015).
54. Y. Zeng *et al.*; Major Depressive Disorder Working Group of the Psychiatric Genomics Consortium, Genome-wide regional heritability mapping identifies a locus within the TOX2 gene associated with major depressive disorder. *Biol. Psychiatry* **82**, 312–321 (2017).
55. C. Luo, P. Hajkova, J. R. Ecker, Dynamic DNA methylation: In the right place at the right time. *Science* **361**, 1336–1340 (2018).
56. M. N. Davies *et al.*, Functional annotation of the human brain methylome identifies tissue-specific epigenetic variation across brain and blood. *Genome Biol.* **13**, R43 (2012).
57. E. Hannon, K. Lunnon, L. Schalkwyk, J. Mill, Interindividual methylomic variation across blood, cortex, and cerebellum: Implications for epigenetic studies of neurological and neuropsychiatric phenotypes. *Epigenetics* **10**, 1024–1032 (2015).
58. E. Walton *et al.*, Correspondence of DNA methylation between blood and brain tissue and its application to schizophrenia research. *Schizophr. Bull.* **42**, 406–414 (2016).
59. P. R. Braun *et al.*, Genome-wide DNA methylation comparison between live human brain and peripheral tissues within individuals. *Transl. Psychiatry* **9**, 47 (2019).
60. N. Provençal *et al.*, The signature of maternal rearing in the methylome in rhesus macaque prefrontal cortex and T cells. *J. Neurosci.* **32**, 15626–15642 (2012).
61. M. W. Logue *et al.*; Traumatic Stress Brain Study Group, An epigenome-wide association study of posttraumatic stress disorder in US veterans implicates several new DNA methylation loci. *Clin. Epigenetics* **12**, 46 (2020).
62. A. Sasaki, M. E. Eng, A. H. Lee, A. Kostaki, S. G. Matthews, DNA methylome signatures of prenatal exposure to synthetic glucocorticoids in hippocampus and peripheral whole blood of female guinea pigs in early life. *Transl. Psychiatry* **11**, 63 (2021).
63. K. Kouter, T. Zupanc, A. Videtič Paska, Targeted sequencing approach: Comprehensive analysis of DNA methylation and gene expression across blood and brain regions in suicide victims. *World J. Biol. Psychiatry* **Mar 9**, 1–12 10.1080/15622975.2022.2046291. (2022).
64. E. Beurel, M. Toups, C. B. Nemeroff, The bidirectional relationship of depression and inflammation: Double trouble. *Neuron* **107**, 234–256 (2020).
65. W. C. Drevets, G. M. Wittenberg, E. T. Bullmore, H. K. Manji, Immune targets for therapeutic development in depression: Towards precision medicine. *Nat. Rev. Drug Discov.* **21**, 224–244 (2022).
66. M. E. Lynall *et al.*; Neuroimmunology of Mood Disorders and Alzheimer's Disease (NIMA) Consortium, Peripheral blood cell-stratified subgroups of inflamed depression. *Biol. Psychiatry* **88**, 185–196 (2020).
67. T. Zhu *et al.*, A pan-tissue DNA methylation atlas enables in silico decomposition of human tissue methylomes at cell-type resolution. *Nat. Methods* **19**, 296–306 (2022).
68. K. G. Coupland *et al.*, DNA methylation of the MAPT gene in Parkinson's disease cohorts and modulation by vitamin E in vitro. *Mov. Disord.* **29**, 1606–1614 (2014).
69. M. L. Molendijk *et al.*, Serum BDNF concentrations as peripheral manifestations of depression: Evidence from a systematic review and meta-analyses on 179 associations (N=9484). *Mol. Psychiatry* **19**, 791–800 (2014).
70. H. Yu, Z. Y. Chen, The role of BDNF in depression on the basis of its location in the neural circuitry. *Acta Pharmacol. Sin.* **32**, 3–11 (2011).
71. K. Fumoto, C. C. Hoogenraad, A. Kikuchi, GSK-3beta-regulated interaction of BICD with dynein is involved in microtubule anchorage at centrosome. *EMBO J.* **25**, 5670–5682 (2006).
72. M. Terenzio *et al.*, Bicaudal-D1 regulates the intracellular sorting and signalling of neurotrophin receptors. *EMBO J.* **33**, 1582–1598 (2014).
73. P. Enríquez, CRISPR-Mediated Epigenome Editing. *Yale J. Biol. Med.* **89**, 471–486 (2016).
74. M. J. Aryee *et al.*, Minfi: A flexible and comprehensive Bioconductor package for the analysis of Infinium DNA methylation microarrays. *Bioinformatics* **30**, 1363–1369 (2014).
75. T. J. Morris *et al.*, ChAMP: 450k chip analysis methylation pipeline. *Bioinformatics* **30**, 428–430 (2014).
76. Y. Benjamini, Y. Hochberg, Controlling the false discovery rate: A practical and powerful approach to multiple testing. *J. R. Stat. Soc. B* **57**, 289–300 (1995).
77. R. Han, Z. Liu, Data and code "Genome-wide profiling of the DNA methylome in the peripheral blood of MDD patients." Gene Expression Omnibus. https://www.ncbi.nlm.nih.gov/geo/query/acc.cgi?acc=GSE201287. Deposited 22 April 2022.
78. F. Du, R. Han, Data and code "Peripheral whole blood: Healthy control and Major depression disorder patients." Gene Expression Omnibus. https://www.ncbi.nlm.nih.gov/geo/query/acc.cgi?acc=GSE201332. Deposited 22 April 2022.